Fractional chemotaxis diffusion equations

T. A. M. Langlands*
Department of Mathematics and Computing, University of Southern Queensland, Toowoomba, Queensland 4350, Australia

B. I. Henry†
Department of Applied Mathematics, School of Mathematics, University of New South Wales, Sydney, New South Wales 2052, Australia

(Received 15 February 2010; published 4 May 2010)

We introduce mesoscopic and macroscopic model equations of chemotaxis with anomalous subdiffusion for modeling chemically directed transport of biological organisms in changing chemical environments with diffusion hindered by traps or macromolecular crowding. The mesoscopic models are formulated using continuous time random walk equations and the macroscopic models are formulated with fractional order differential equations. Different models are proposed depending on the timing of the chemotactic forcing. Generalizations of the models to include linear reaction dynamics are also derived. Finally a Monte Carlo method for simulating anomalous subdiffusion with chemotaxis is introduced and simulation results are compared with numerical solutions of the model equations. The model equations developed here could be used to replace Keller-Segel type equations in biological systems with transport hindered by traps, macromolecular crowding or other obstacles.

DOI: 10.1103/PhysRevE.81.051102 PACS number(s): 05.40.Fb, 02.70.Bf, 87.17.Jj, 05.10.Gg

I. INTRODUCTION

Diffusion and chemotaxis are fundamental to the motion of bacteria [1], the directed motion of neutrophils in response to infection [2], hypoxia stimulated angiogenesis [3] and many other biological transport processes [2]. These transport processes can further be complicated by traps [4], macromolecular crowding [5] or other obstacles resulting in anomalous subdiffusion characterized by an ensemble averaged mean square displacement of diffusing species, $\langle r^2(t)\rangle$, that scales sublinearly in time, i.e., $\langle r^2(t)\rangle \sim t^\gamma$ with $0<\gamma<1$ [6–17]. In this paper we introduce mesoscopic and macroscopic models for transport in biological systems with chemotaxis and anomalous subdiffusion.

The classic macroscopic model for the evolution of a diffusing species, with concentration $n(x,t)$, in the presence of a chemoattractant, with concentration $c(x,t)$, is the Keller-Segel model [18]

$$\frac{\partial n}{\partial t} = D\frac{\partial^2 n}{dx^2} - \chi\frac{\partial}{\partial x}\left(n\frac{\partial c}{\partial x}\right), \tag{1}$$

where D and χ denote the diffusion coefficient and the chemotactic coefficient respectively. In this model if the chemoattractant is removed the evolution corresponds to standard Brownian diffusion with $\langle r^2(t)\rangle \sim t$.

Anomalous subdiffusion can be modeled as fractional Brownian motion (fBm) [19–21] or continuous time random walks (CTRWs) [22,23] with long-tailed waiting-time densities [13]. Both of these models are non-Markovian and both exhibit the same sublinear scaling for the ensemble averaged mean square displacement. However the second moment of the velocity scales differently in the two models [24] and the time averaged mean square displacement differs from the ensemble averaged mean square displacements in the CTRW model, but not in the fBm model [25]. Both possibilities should be considered when interpreting results from experiments using single particle tracking [25] or fluorescence recovery after photobleaching [26] and a simple test has been devised for analyzing experimental data to determine which model is most appropriate [27].

At the macroscopic level, anomalous subdiffusion can be modeled through a modified diffusion equation

$$\frac{\partial C}{\partial t} = \mathcal{D}(\gamma,t)\nabla^2 C \tag{2}$$

with the diffusion constant replaced by a fractional temporal operator. In the case of fractional Brownian motion (fBm) this operator is given by [20,21]

$$\mathcal{D}_I(\gamma,t) = D(\gamma)\gamma t^{\gamma-1}. \tag{3}$$

In the CTRW model [22], with power law waiting times [13], the fractional temporal operator is given by

$$\mathcal{D}_{II}(\gamma,t) = D(\gamma)\frac{\partial^{1-\gamma}}{\partial t^{1-\gamma}}, \tag{4}$$

where $D(\gamma)$ is a generalized diffusion coefficient with units of $\mathrm{m}^2\ \mathrm{s}^{-\gamma}$ and

$$\frac{\partial^{1-\gamma}}{\partial t^{1-\gamma}}Y(t) = \frac{1}{\Gamma(\gamma)}\frac{\partial}{\partial t}\int_0^t \frac{Y(t')}{(t-t')^{1-\gamma}}dt' \tag{5}$$

defines the Riemann-Liouville fractional derivative of non-integer order $1-\gamma$ for $0<\gamma<1$.

The fractional derivative is an integer order derivative of the fractional integral

$$\frac{\partial^{-\gamma}}{\partial t^{-\gamma}}Y(t) = \frac{1}{\Gamma(\gamma)}\int_0^t \frac{Y(t')}{(t-t')^{1-\gamma}}dt', \tag{6}$$

which itself is a generalization of the Cauchy formula

*t.langlands@usq.edu.au
†b.henry@unsw.edu.au

$$\frac{d^{-n}Y(t)}{dt^{-n}} = \int_0^t \left(\int_0^{t_{n-1}} \cdots \left\{ \int_0^{t_2} \left[\int_0^{t_1} Y(t_0) dt_0 \right] dt_1 \right\} \cdots \right) dt_{n-1}$$
$$= \frac{1}{\Gamma(n)} \int_0^t \frac{Y(t')}{(t-t')^{1-n}} dt'$$

for noninteger n. The fractional integral, Eq. (6), defines a power law weighted average of the function $Y(t)$.

There have been various attempts to modify the fractional macroscopic diffusion equations to include force fields and reactions [13,28]. The Fokker-Planck equation for diffusion in a force field can readily be generalized by replacing the diffusion coefficient with a time dependent fractional operator as above. This has been justified within the framework of CTRWs, for force fields that vary in space but not time [13,29] and for force fields that vary in time but not space [30]. However these derivations do not extend to the more general case of anomalous subdiffusion in a general external force field $f(x,t)$ that varies in both time and space. Two obvious possible generalizations in this case are [31]

$$\frac{\partial n}{\partial t} = \frac{\partial^{1-\gamma}}{\partial t^{1-\gamma}} D_\gamma \nabla^2 n - \frac{1}{\eta_\gamma} \frac{\partial^{1-\gamma}}{\partial t^{1-\gamma}} \nabla [f(x,t) n(x,t)] \tag{7}$$

and [32–34]

$$\frac{\partial n}{\partial t} = \frac{\partial^{1-\gamma}}{\partial t^{1-\gamma}} D_\gamma \nabla^2 n - \frac{1}{\eta_\gamma} \nabla \left(f(x,t) \frac{\partial^{1-\gamma}}{\partial t^{1-\gamma}} n(x,t) \right). \tag{8}$$

If the force field is purely space dependent then the two models are equivalent and the solution is time subordinated to the concentration of diffusing species in the standard Fokker-Planck equation. This temporal subordination is not physically appropriate for time dependent external force fields [32]. However an alternate formulation using an Ito stochastic differential equation has been proposed with a modified subordination in which the force varies in real time rather than the random time [33]. In chemotaxis there may be a physical link between the time scale of the diffusion and the time scale of the effective force field since the latter depends on the concentration of another diffusing species. Similarly in the fractional Nernst-Planck equation considered in [35,36] the force field from the membrane potential depends on concentrations of the diffusing species.

In Sec. II we introduce four different models of chemotaxis with anomalous subdiffusion. The different models are characterized by differences in the nature of the anomalous diffusion (fBm or power law CTRWs), and differences in the details of the underlying random walk processes.

In Sec. III numerical solutions of the associated discrete space equations are obtained for each model. The numerical results are compared with Monte Carlo random walk simulations, with chemotactic forcing, on the same grid and using the same parameters. Differences between the model results are discussed in Sec. IV.

II. FRACTIONAL CHEMOTAXIS DIFFUSION MODELS

A. Model I

To model chemotaxis with fractional Brownian motion we consider an *ad-hoc* model in which we replace both the diffusion coefficient and the chemotactic coefficient by fractional temporal operators as in Eq. (3). This yields

$$\frac{\partial n}{\partial t} = \gamma t^{\gamma-1} \left[D_\gamma \frac{\partial^2 n}{\partial x^2} - \chi_\gamma \frac{\partial}{\partial x} \left(n \frac{\partial c}{\partial x} \right) \right], \tag{9}$$

where γ is the anomalous diffusion exponent, D_γ is the anomalous diffusion coefficient (with units $\mathrm{m}^2\ \mathrm{s}^{-\gamma}$), and χ_γ is the analogous anomalous chemotaxis coefficient. This model equation reduces to the standard Keller-Segel chemotaxis equation, Eq. (1), when $\gamma=1$.

B. Model II

A simple model for chemotaxis with fractional diffusion from power law CTRWs starts with the equation

$$n_i(t) = n_i(0)\Phi(t) + \int_0^t \{ p_r(x_{i-1},t') n_{i-1}(t') + p_l(x_{i+1},t') n_{i+1}(t') \} \psi(t-t') dt', \tag{10}$$

where $\psi(t)$ is a (power law) waiting-time density,

$$\Phi(t) = \int_t^\infty \psi(t') dt' \tag{11}$$

is the corresponding survival probability, and $p_r(x,t)$ and $p_l(x,t)$ are the probabilities of jumping from x to the adjacent grid point to the right and left directions, respectively. Equation (10) can be derived from the CTRW formalism (see e.g., [28]) if and only if the jumping porbabilities do not depend on time. Our inclusion of time dependence is an *ad hoc* generalization in this sense. The physical interpretation of Eq. (10) is that the number of particles at grid point i at time t is comprised of those particles that were at point i at time $t=0$ which have not yet jumped (the first term on the right hand side) together with those particles that were at an adjacent grid point $i \pm 1$ at an earlier time t' but then jumped to point i at time t after waiting a time $t-t'$. The probabilities $p_r(x,t)$ and $p_l(x,t)$ are dependent on the chemoattractant concentrations, $c(x,t)$, at the neighboring points of the point x at time t. Equation (10) is a continuous time representation of the transition probability law in [37].

Following Stevens [37], the probabilities of jumping to the left or right direction are based on the proportion of the chemoattractant on either side of the current point via

$$p_l(x_i,t) = \frac{v(x_{i-1},t)}{v(x_{i-1},t) + v(x_{i+1},t)}, \tag{12}$$

and

$$p_r(x_i,t) = \frac{v(x_{i+1},t)}{v(x_{i-1},t) + v(x_{i+1},t)}, \tag{13}$$

where $v(x,t)$ is a sensitivity function that depends on the concentration of the chemoattractant,

$$v(x,t) = \exp[\beta c(x,t)]. \tag{14}$$

Note that with the above we have

$$p_l(x_i,t) + p_r(x_i,t) = 1 \tag{15}$$

and

$$p_l(x_i,t) - p_r(x_i,t) = \frac{e^{\beta c(x_{i-1},t)} - e^{\beta c(x_{i+1},t)}}{e^{\beta c(x_{i-1},t)} + e^{\beta c(x_{i+1},t)}}. \tag{16}$$

Using the notation $\mathcal{L}\{f(t)\}(s)$ or $\hat{f}(s)$ to denote the Laplace transform with respect to time of a function $f(t)$ we have the Laplace transform of Eq. (10),

$$\hat{n}_i(s) = n_i(0)\hat{\Phi}(s) + \{\mathcal{L}\{p_r(x_{i-1},t)n_{i-1}(t)\}(s) + \mathcal{L}\{p_l(x_{i+1},t)n_{i+1}(t)\}(s)\}\hat{\psi}(s). \tag{17}$$

Using the identity

$$\hat{\Phi}(s) = [1 - \hat{\psi}(s)]/s, \tag{18}$$

which follows from the Laplace transform of Eq. (11), we have

$$s\hat{n}_i(s) - n_i(0) = \frac{\hat{\psi}(s)}{\hat{\Phi}(s)}\{-\hat{n}_i(s) + \mathcal{L}\{p_r(x_{i-1},t)n_{i-1}(t)\}(s) + \mathcal{L}\{p_l(x_{i+1},t)n_{i+1}(t)\}(s)\}. \tag{19}$$

We now consider a heavy-tailed waiting-time density which behaves for long times as

$$\psi(t) \sim \frac{\kappa}{\tau}\left(\frac{t}{\tau}\right)^{-1-\gamma}, \tag{20}$$

where γ is the anomalous exponent, τ is the characteristic waiting-time, and κ is a dimensionless constant. Using a Tauberian (Abelian) theorem [38] we can write the Laplace transform for this density function as (for small s)

$$\hat{\psi}(s) \sim 1 - \frac{\kappa\Gamma(1-\gamma)}{\gamma}(s\tau)^{\gamma}. \tag{21}$$

Using Eq. (18), we then find the corresponding asymptotic form for the survival probability

$$\hat{\Phi}(s) \sim \frac{\kappa\Gamma(1-\gamma)}{\gamma}\tau^{\gamma}s^{\gamma-1} \tag{22}$$

and the ratio

$$\frac{\hat{\psi}(s)}{\hat{\Phi}(s)} \sim A_\gamma \frac{s^{1-\gamma}}{\tau^{\gamma}}, \tag{23}$$

where

$$A_\gamma = \frac{\gamma}{\kappa\Gamma(1-\gamma)}.$$

Specific cases of waiting-time densities are the Mittag-Leffler density [39]

$$\psi(t) = -\frac{d}{dt}E_\gamma\left[-\left(\frac{t}{\tau}\right)^{\gamma}\right], \tag{24}$$

where $E_\gamma(z)$ is the Mittag-Leffler function [40], and the Pareto law used by [41]

$$\psi(t) = \frac{\gamma/\tau}{(1+t/\tau)^{1+\gamma}}. \tag{25}$$

The corresponding values for A_γ can be shown to be

$$A_\gamma = 1 \quad \text{and} \quad A_\gamma = \frac{1}{\Gamma(1-\gamma)} \tag{26}$$

for Eqs. (24) and (25), respectively. Note the ratio in Eq. (23) is only valid long times for the Pareto density, Eq. (25), while it is exact for the Mittag-Leffler density for all times. In addition, if $\gamma=1$ we do not use Eq. (25) but instead use Eq. (24).

With Eq. (23), Eq. (19) now becomes

$$s\hat{n}_i(s) - n_i(0) = \frac{A_\gamma s^{1-\gamma}}{\tau^{\gamma}}\{-\hat{n}_i(s) + \mathcal{L}\{p_r(x_{i-1},t)n_{i-1}(t)\}(s) + \mathcal{L}\{p_l(x_{i+1},t)n_{i+1}(t)\}(s)\}. \tag{27}$$

Noting that the Laplace Transform of a Riemann-Liouville fractional derivative of order α, where $0<\alpha\leq 1$, is given by [40]

$$\mathcal{L}\left\{\frac{d^\alpha f(t)}{dt^\alpha}\right\}(s) = s^\alpha\hat{f}(s) - \left[\frac{d^{\alpha-1}f(t)}{dt^{\alpha-1}}\right|_{t=0} \tag{28}$$

we can invert the Laplace transforms in Eq. (27) to obtain

$$\frac{dn_i}{dt} = \frac{A_\gamma}{\tau^\gamma}\frac{d^{1-\gamma}}{dt^{1-\gamma}}\{-n_i(t) + p_r(x_{i-1},t)n_{i-1}(t) + p_l(x_{i+1},t)n_{i+1}(t)\}, \tag{29}$$

where we have ignored the last term in Eq. (28). Numerical solutions of this discrete space fractional differential equation for Model II are considered in Sec. III.

The spatial continuum limit of Model II can be obtained in the usual way by setting $x_i=x$ and $x_{i\pm1}=x\pm\Delta x$ and carrying out Taylor series expansions in x. Retaining terms to order $(\Delta x)^2$ and using the normalization $p_l(x,t)+p_r(x,t)=1$ we first find that

$$-n_i(t) + p_r(x_{i-1},t)n_{i-1}(t) + p_l(x_{i+1},t)n_{i+1}(t) = \Delta x\frac{\partial}{\partial x}\{n(x,t)[p_l(x,t) - p_r(x,t)]\} + \frac{\Delta x^2}{2}\frac{\partial^2}{\partial x^2}n(x,t). \tag{30}$$

This simplifies further after carrying out Taylor series expansions in Eq. (16), to arrive at

$$p_l(x,t) - p_r(x,t) \approx \frac{e^{-\beta\Delta x\partial c/\partial x} - e^{\beta\Delta x\partial c/\partial x}}{e^{-\beta\Delta x\partial c/\partial x} + e^{\beta\Delta x\partial c/\partial x}},$$

$$= -\tanh\left(\beta\Delta x\frac{\partial c}{\partial x}\right),$$

$$\approx -\beta\Delta x\frac{\partial c}{\partial x}. \tag{31}$$

We can now combine the results in Eq. (30) and Eq. (31) with Eq. (29) to obtain

$$\frac{\partial n}{\partial t} \simeq \frac{\partial^{1-\gamma}}{\partial t^{1-\gamma}}\left[\frac{A_\gamma \Delta x^2}{2\tau^\gamma}\frac{\partial^2 n}{\partial x^2}(x,t) - \frac{A_\gamma \beta \Delta x^2}{\tau^\gamma}\frac{\partial}{\partial x}\left(\frac{\partial c(x,t)}{\partial x}n(x,t)\right)\right] + O(\Delta x^4) \tag{32}$$

and then taking the limit $\Delta x \to 0$ and $\tau \to 0$, with

$$D_\gamma = \frac{A_\gamma \Delta x^2}{2\tau^\gamma} \tag{33}$$

and

$$\chi_\gamma = \frac{A_\gamma \beta \Delta x^2}{\tau^\gamma}, \tag{34}$$

we have

$$\frac{\partial n}{\partial t} = \frac{\partial^{1-\gamma}}{\partial t^{1-\gamma}}\left[D_\gamma \frac{\partial^2 n(x,t)}{\partial x^2} - \chi_\gamma \frac{\partial}{\partial x}\left(\frac{\partial c(x,t)}{\partial x}n(x,t)\right)\right]. \tag{35}$$

Equation (35) provides a useful approximation for the space and time evolution of the concentration of an anomalously diffusing species that is chemotactically attracted by another species. In Eq. (10) the probabilities to jump left or right are determined at the start of the waiting times. We will consider another model in Sec. II D where the probabilities to jump left or right are determined at the end of the waiting times. But first, in the next section, we consider a more rigorous formulation, based on the generalized master equation approach.

C. Model III

In this section we follow the generalized master equation approach of [30,42,43], extended to take into account the effect of the chemoattractant. To begin we write the balance equation for the concentration of particles, n, at the site i

$$\frac{dn_i(t)}{dt} = J_i^+(t) - J_i^-(t), \tag{36}$$

where $J_i^\pm$ are the gain (+) and loss (−) fluxes at the site i. We also have the conservation equation for the arriving flux of particles at the point i given by the flux of particles either leaving the site $i-1$ and jumping to the right or leaving the site $i+1$ that move to the left,

$$J_i^+(t) = p_r(x_{i-1},t)J_{i-1}^-(t) + p_l(x_{i+1},t)J_{i+1}^-(t), \tag{37}$$

where $p_l(x,t)$ and $p_r(x,t)$ are given in Eqs. (12) and (13). We can combine Eqs. (37) and (36) to obtain an evolution law for the concentration purely in terms of the loss flux, viz;

$$\frac{dn_i(t)}{dt} = p_r(x_{i-1},t)J_{i-1}^-(t) + p_l(x_{i+1},t)J_{i+1}^-(t) - J_i^-(t). \tag{38}$$

The loss flux at the site i is given by

$$J_i^-(t) = \psi(t)n_i(0) + \int_0^t \psi(t-t')J_i^+(t')dt'. \tag{39}$$

The first term represents those particles that were originally at i at $t=0$ and wait until time t when they leave. The second term represents particles that arrived at some earlier time t' and wait until time t to leave. Here $\psi(t)$ is the usual waiting-time density used in Model II. We can combine Eqs. (36) and (39) to obtain

$$J_i^-(t) = \psi(t)n_i(0) + \int_0^t \psi(t-t')\left[J_i^-(t') + \frac{dn_i(t')}{dt}\right]dt' \tag{40}$$

and then we can solve for the loss flux using Laplace transform methods. The Laplace transform of Eq. (40) with respect to time yields

$$\hat{J}_i^-(s) = \hat{\psi}(s)n_i(0) + \hat{\psi}(s)[\hat{J}_i^-(s) + s\hat{n}_i(s) - n_i(0)], \tag{41}$$

which simplifies further as

$$\hat{J}_i^-(s) = \frac{\hat{\psi}(s)}{\hat{\Phi}(s)}\hat{n}_i(s). \tag{42}$$

Now using the approximation in Eq. (23) for a heavy-tailed waiting-time density and inverting the Laplace transform we have

$$J_i^-(t) = \frac{A_\gamma}{\tau^\gamma}\frac{d^{1-\gamma}n_i(t)}{dt^{1-\gamma}}. \tag{43}$$

It follows from Eqs. (38) and (43) that the evolution equation for the particle density in Mode II, Eq. (29), is the evolution equation for the loss flux in Model III. We now substitute the expression for the loss flux, Eq. (43) back into the balance equation, Eq. (38), to obtain

$$\frac{dn_i(t)}{dt} = \frac{A_\gamma}{\tau^\gamma}\left\{p_r(x_{i-1},t)\frac{d^{1-\gamma}n_{i-1}(t)}{dt^{1-\gamma}} + p_l(x_{i+1},t)\frac{d^{1-\gamma}n_{i+1}(t)}{dt^{1-\gamma}} - \frac{d^{1-\gamma}n_i(t)}{dt^{1-\gamma}}\right\}. \tag{44}$$

Numerical solutions of this discrete space fractional differential equation for Model III are considered in Sec. III.

The continuous space representation of Eq. (44) is found by setting $x_i = x$ and $x_{i\pm1} = x \pm \Delta x$ so that

$$\frac{\partial n(x,t)}{\partial t} = \frac{A_\gamma}{\tau^\gamma}\left\{p_r(x-\Delta x,t)\frac{\partial^{1-\gamma}n(x-\Delta x,t)}{\partial t^{1-\gamma}} + p_l(x+\Delta x,t)\frac{\partial^{1-\gamma}n(x+\Delta x,t)}{\partial t^{1-\gamma}} - \frac{\partial^{1-\gamma}n(x,t)}{\partial t^{1-\gamma}}\right\}. \tag{45}$$

The continuum limit representation can then be found by carrying out Taylor series expansions about x, similar to the steps used to reduce Eq. (29) to Eq. (35). This results in the equation

$$\frac{\partial n}{\partial t} = \frac{\partial^{1-\gamma}}{\partial t^{1-\gamma}}D_\gamma \frac{\partial^2 n(x,t)}{\partial x^2} - \chi_\gamma \frac{\partial}{\partial x}\left(\frac{\partial c(x,t)}{\partial x}\frac{\partial^{1-\gamma}n(x,t)}{\partial t^{1-\gamma}}\right). \tag{46}$$

Model II and Model III are similar to the fractional Fokker Planck equations, Eqs. (7) and (8), respectively, with forcing from the chemotactic gradient $\frac{\partial c(x,t)}{\partial x}$.

D. Model IV

We now reconsider Model II but with the jump probabilities calculated after the particle has waited and immediately prior to jumping. The governing equation in this case is given by

$$n_i(t) = n_i(0)\Phi(t) + p_r(x_{i-1},t)\int_0^t n_{i-1}(t')\psi(t-t')dt' + p_l(x_{i+1},t)\int_0^t n_{i+1}(t')\psi(t-t')dt'. \quad (47)$$

It is convenient to introduce the auxiliary function

$$m_i(t) = \int_0^T n_i(t')\psi(t-t')dt', \quad (48)$$

which has the Laplace transform

$$\hat{m}_i(s) = \hat{n}_i(s)\hat{\psi}(s). \quad (49)$$

The Laplace transform of Eq. (47) with respect to time can then be written as

$$(s\hat{n}_i(s) - n_i(0))\hat{\Phi}(s) = -\hat{\psi}(s)\hat{n}_i(s) + \mathcal{L}\{p_r(x_{i-1},t)m_{i-1}(t)\}(s) + \mathcal{L}\{p_l(x_{i+1},t)m_{i+1}(t)\}(s), \quad (50)$$

and after the inverse Laplace transform,

$$\int_0^t \frac{\partial n_i}{\partial t'}\Phi(t-t')dt' = m_i(t) + p_r(x_{i-1},t)m_{i-1}(t) + p_l(x_{i+1},t)m_{i+1}(t). \quad (51)$$

Proceeding to the continuum limit with Taylor series expansions about x, similar to the steps in Model II and Model III, we obtain

$$\int_0^t \Phi(t-t')\frac{\partial n(x,t')}{\partial t}dt' \simeq \frac{\Delta x^2}{2}\frac{\partial^2 m(x,t)}{\partial x^2} - \Delta x^2\beta\frac{\partial}{\partial x}\left(\frac{\partial c(x,t)}{\partial x}m(x,t)\right) + O(\Delta x^4), \quad (52)$$

and then using the auxiliary function definition in Eq. (48) we find

$$\int_0^t \Phi(t-t')\frac{\partial n(x,t')}{\partial t}dt' \simeq \frac{\Delta x^2}{2}\int_0^t \frac{\partial^2 n(x,t')}{\partial x^2}\psi(t-t')dt' - \Delta x^2\beta\frac{\partial}{\partial x}\left(\frac{\partial c(x,t)}{\partial x}\int_0^t n(x,t')\psi(t-t')dt'\right) + O(\Delta x^4). \quad (53)$$

Asymptotic expressions for the convolution integrals in Eq. (53) can be obtained by considering asymptotic expansions in Laplace space and then inverting. Thus we now consider the terms

$$\mathcal{L}\left\{\int_0^t \Phi(t-t')\frac{\partial n(x,t')}{\partial t}dt'\right\}(s) = \hat{\Phi}(s)\mathcal{L}\left\{\frac{\partial n(x,t)}{\partial t}\right\}(s), \quad (54)$$

$$\mathcal{L}\left\{\int_0^t \frac{\partial^2 n(x,t')}{\partial x^2}\psi(t-t')dt'\right\}(s) = \hat{\psi}(s)\frac{\partial^2 \hat{n}(x,s)}{\partial x^2}, \quad (55)$$

$$\mathcal{L}\left\{\int_0^t n(x,t')\psi(t-t')dt'\right\}(s) = \hat{\psi}(s)\hat{n}(x,s). \quad (56)$$

For long times (small s) we have, with the use of Eqs. (21) and (22)

$$\hat{\Phi}(s) \simeq \frac{s^{\gamma-1}\tau^\gamma}{A_\gamma} + O(s^{2\gamma-1}), \quad (57)$$

$$\hat{\psi}(s) \simeq 1 - \frac{(s\tau)^\gamma}{A_\gamma} + O(s^\gamma). \quad (58)$$

Using these expansions in Eqs. (54)–(56) and taking the inverse Laplace transforms to replace the convolution integrals in Eq. (53) we obtain

$$\frac{\tau^\gamma}{A_\gamma}\frac{\partial^{\gamma-1}}{\partial t^{\gamma-1}}\frac{\partial n(x,t)}{\partial t} \simeq \frac{\Delta x^2}{2}\frac{\partial^2 n(x,t)}{\partial x^2} - \Delta x^2\beta\frac{\partial}{\partial x}\left(\frac{\partial c(x,t)}{\partial x}n(x,t)\right) + O(\Delta x^4), \quad (59)$$

and in the limit $\Delta x \to 0$ and $\tau \to 0$

$$\frac{\partial n(x,t)}{\partial t} = \frac{\partial^{1-\gamma}}{\partial t^{1-\gamma}}\left[D_\gamma\frac{\partial^2 n(x,t)}{\partial x^2} - \chi_\gamma\frac{\partial}{\partial x}\left(\frac{\partial c(x,t)}{\partial x}n(x,t)\right)\right] \quad (60)$$

as previously in Eq. (35).

Conversely, for short times (large s) we have

$$\hat{\Phi}(s) \simeq \frac{1}{s} + O(s^{-\nu_\gamma-1}), \quad (61)$$

$$\hat{\psi}(s) \simeq \frac{B_\gamma s^{-\nu_\gamma}}{\tau^{\nu_\gamma}} + O(s^{-2\nu_\gamma}), \quad (62)$$

where $\nu_\gamma = \gamma$ and $B_\gamma = 1$ if use the Mittag-Leffler [Eq. (24)] and $\nu_\gamma = 1$ and $B_\gamma = \gamma$ if we use the Pareto [Eq. (25)] density. The resulting equation for Eq. (53) becomes for short times

$$\frac{\partial n(x,t)}{\partial t} = D^*_\gamma\frac{\partial^{1-\nu_\gamma}}{\partial t^{1-\nu_\gamma}}\frac{\partial^2 n(x,t)}{\partial x^2} - \chi^*_\gamma\frac{\partial}{\partial x}\frac{\partial}{\partial t}\left(\frac{\partial c(x,t)}{\partial x}\frac{\partial^{-\nu}\gamma n(x,t)}{\partial t^{-\nu_\gamma}}\right) \quad (63)$$

with the modified coefficients

$$D^*_\gamma = \frac{B_\gamma\Delta x^2}{2\tau^{\nu_\gamma}} \quad (64)$$

and

$$\chi_\gamma^* = \frac{B_\gamma \beta \Delta x^2}{\tau^{\nu_\gamma}}. \tag{65}$$

In the case of the Mittag-Leffler density [Eq. (24)], the short-time equation can be simplified to

$$\frac{\partial n(x,t)}{\partial t} = D_\gamma^* \frac{\partial^{1-\gamma}}{\partial t^{1-\gamma}} \frac{\partial^2 n(x,t)}{\partial x^2} - \chi_\gamma \frac{\partial}{\partial x}\left(\frac{\partial c(x,t)}{\partial x} \frac{\partial^{1-\gamma} n(x,t)}{\partial t^{1-\gamma}} \right) - \chi_\gamma^* \frac{\partial}{\partial x}\left(\frac{\partial^2 c(x,t)}{\partial x\, \partial t} \frac{\partial^{-\gamma} n(x,t)}{\partial t^{-\gamma}} \right). \tag{66}$$

Equation (66) is similar to the governing equation of Model III given by Eq. (46) except for the last term. However this term will be close to zero at short times so the two equations are asymptotically equivalent in this short time limit. Conversely if we use the Pareto density [Eq. (25)] then Eq. (63) becomes

$$\frac{\partial n(x,t)}{\partial t} = \gamma D_1 \frac{\partial^2 n(x,t)}{\partial x^2} - \gamma \chi_1 \frac{\partial}{\partial x}\left(\frac{\partial c(x,t)}{\partial x} n(x,t) \right) - \gamma \chi_1 \frac{\partial}{\partial x}\left(\frac{\partial^2 c(x,t)}{\partial x\, \partial t} \frac{\partial^{-1} n(x,t)}{\partial t^{-1}} \right). \tag{67}$$

If we again consider the last term to be small then the resulting equation is similar to the standard chemotaxis Eq. (1), apart from the multiplicative factor γ that multiplies each term on the right hand side. The effect of this multiplicative factor is to slow the initial temporal behavior of the solution (linear rescaling).

Note that if we use the Mittag-Leffler density in Eq. (24) then we see that the mesoscopic equation Eq. (47) bridges the gap between Model II and Model III. At short times it recovers Model III, Eq. (46), whereas at long times it recovers Model II [Eq. (35)]. The latter shows that for long times, compared to the characteristic time τ, there is no difference between evaluating the chemotactic probabilities at the time before or after the particle waits.

III. FRACTIONAL CHEMOTAXIS REACTION-DIFFUSION MODELS

In this section we consider extensions of the CTRW based fractional chemotaxis diffusion models to incorporate reactions. In the absence of chemotaxis, extensions of CTRW based fractional diffusion models to include linear reactions were derived in [44,45] and extensions to include nonlinear reactions were derived in [46,47].

A. Model II

Following the approach in [44] we can incorporate reactions in CTRW models by increasing or decreasing the concentration of particles during the waiting times by an amount proportional to the evolution operator for the reaction dynamics. The governing equation for Model II with linear reaction dynamics incorporated in this way becomes

$$n_i(t) = e^{kt} n_i(0) \Phi(t) + \int_0^t \{ p_r(x_{i-1},t') n_{i-1}(t') + p_l(x_{i+1},t') n_{i+1}(t') \} e^{k(t-t')} \psi(t-t')\, dt', \tag{68}$$

where k is the per capita rate gain ($k>0$) or loss ($k<0$) of particles. Again Laplace transform methods can be used to convert the integral equation representation into a (fractional) differential equation. The Laplace transform of Eq. (68) with respect to time yields

$$\hat{n}_i(s) = n_i(0) \hat{\Phi}(s-k) + \mathcal{L}\{p_r(x_{i-1},t) n_{i-1}(t)\}(s) \hat{\psi}(s-k) + \mathcal{L}\{p_l(x_{i+1},t) n_{i+1}(t)\}(s) \hat{\psi}(s-k), \tag{69}$$

and after rearranging we find

$$s\hat{n}_i(s) - n_i(0) = k\hat{n}_i(s) + \frac{\hat{\psi}(s-k)}{\hat{\Phi}(s-k)} \{ -\hat{n}_i(s) + \mathcal{L}\{p_r(x_{i-1},t) n_{i-1}(t)\} \times (s) + \mathcal{L}\{p_l(x_{i+1},t) n_{i+1}(t)\}(s) \}, \tag{70}$$

where we have used Eq. (18). With the result in Eq. (23) we can inverting the Laplace transform to obtain

$$\frac{dn_i}{dt} = e^{kt} \frac{A_\gamma}{\tau^\gamma} \frac{d^{1-\gamma}}{dt^{1-\gamma}} \{ e^{-kt} [-n_i(t) + p_r(x_{i-1},t) n_{i-1}(t) + p_l(x_{i+1},t) n_{i+1}(t)] \} + k n_i(t), \tag{71}$$

where the Riemann-Liouville fractional derivative has been replaced by a modified fractional derivative [44,45].

The continuum limit, found by taking Taylor series expansions about x, is

$$\frac{\partial n}{\partial t} = e^{kt} \frac{\partial^{1-\gamma}}{\partial t^{1-\gamma}} \left(e^{-kt} \left\{ D_\gamma \frac{\partial^2 n(x,t)}{\partial x^2} - \chi_\gamma \frac{\partial}{\partial x} \left[\frac{\partial c(x,t)}{\partial x} n(x,t) \right] \right\} \right) + k n(x,t). \tag{72}$$

We note if $n(x,t)$ is not self-chemotactic then the solution of Eq. (72) is given by $n(x,t) = e^{kt} y(x,t)$ where $y(x,t)$ is the solution of Eq. (35) with y replacing n.

B. Model III

To incorporate reactions in Model III we start by modifying Eq. (36) to

$$\frac{dn_i(t)}{dt} = J_i^+(t) - J_i^-(t) + k n_i(t), \tag{73}$$

where k, again, is the per capita rate gain ($k>0$) or loss ($k<0$) of particles. We also modify the expression for the loss flux, $J_i^-(t)$, in Eq. (39) to

$$J_i^-(t) = e^{kt} \psi(t) n_i(0) + \int_0^t e^{k(t-t')} \psi(t-t') J_i^+(t')\, dt', \tag{74}$$

where the exponential factors take into account the per capita addition or removal of particles as in [44].

Now solving for the gain flux, $J_i^+(t)$, in Eq. (73) we find

$$J_i^+(t) = J_i^-(t) + \frac{dn_i(t)}{dt} - kn_i(t) \tag{75}$$

and using Eq. (74) gives

$$J_i^-(t) = e^{kt}\psi(t)n_i(0) + \int_0^t e^{k(t-t')}\psi(t-t') \times \left[J_i^-(t') + \frac{dn_i(t')}{dt} - kn_i(t') \right] dt'. \tag{76}$$

Now using Laplace transform theory we find

$$\hat{J}_i^-(s) = \hat{\psi}(s-k)n_i(0) + \hat{\psi}(s-k)[\hat{J}_i^-(s) + s\hat{n}_i(s) - n_i(0) - k\hat{n}_i(s)] \tag{77}$$

and upon solving for the flux, we find a similar expression to Eq. (42),

$$\hat{J}_i^-(s) = \frac{\hat{\psi}(s-k)}{\hat{\Phi}(s-k)}\hat{n}_i(s). \tag{78}$$

This Laplace transform can now be inverted to find the loss flux given by the modified fractional derivative [44,45] of the concentration at i,

$$J_i^-(t) = e^{kt}\frac{A_\gamma}{\tau^\gamma}\frac{d^{1-\gamma}}{dt^{1-\gamma}}[e^{-kt}n_i(t)], \tag{79}$$

where A_γ is a constant given by 1 or $1/\Gamma(1-\gamma)$ if we use the waiting-time density in Eqs. (24) or (25), respectively.

Now using Eqs. (37) and (79) in Eq. (73) we find

$$\frac{dn_i(t)}{dt} = p_r(x_{i-1},t)e^{kt}\frac{A_\gamma}{\tau^\gamma}\frac{d^{1-\gamma}}{dt^{1-\gamma}}[e^{-kt}n_{i-1}(t)] + p_l(x_{i+1},t)e^{kt}\frac{A_\gamma}{\tau^\gamma}\frac{d^{1-\gamma}}{dt^{1-\gamma}}[e^{-kt}n_{i+1}(t)] - e^{kt}\frac{A_\gamma}{\tau^\gamma}\frac{d^{1-\gamma}}{dt^{1-\gamma}}[e^{-kt}n_i(t)] + kn_i(t). \tag{80}$$

The continuum limit following from setting $x_i = x$, $x_{i\pm1} = x \pm \Delta x$, and Taylor series expansions about x, is given by

$$\frac{\partial n}{\partial t} = D_\gamma e^{kt}\frac{\partial^{1-\gamma}}{\partial t^{1-\gamma}}\left(e^{-kt}\frac{\partial^2 n(x,t)}{\partial x^2} \right) - \chi_\gamma \frac{\partial}{\partial x}\left(\frac{\partial c(x,t)}{\partial x} e^{kt}\frac{\partial^{1-\gamma}}{\partial t^{1-\gamma}}(e^{-kt}n(x,t)) \right) + kn(x,t). \tag{81}$$

C. Model IV

The governing equation for Model IV, Eq. (47), modified to include linear reaction dynamics is given by

$$n_i(t) = e^{kt}n_i(0)\Phi(t) + p_r(x_{i-1},t)\int_0^t n_{i-1}(t')e^{k(t-t')}\psi(t-t')dt' + p_l(x_{i+1},t)\int_0^t n_{i+1}(t')e^{k(t-t')}\psi(t-t')dt'. \tag{82}$$

Following similar steps used to simplify Eq. (47) and using Taylor series expansions we find

$$\int_0^t e^{k(t-t')}\Phi(t-t')\frac{\partial n(x,t')}{\partial t}dt' \simeq \frac{\Delta x^2}{2}\int_0^t \frac{\partial^2 n(x,t')}{\partial x^2}e^{k(t-t')}\psi(t-t')dt' + k\int_0^t e^{k(t-t')}\Phi(t-t')n(x,t')dt' - \Delta x^2\beta\frac{\partial}{\partial x}\left(\frac{\partial c(x,t)}{\partial x}\int_0^t n(x,t')e^{k(t-t')}\psi(t-t')dt' \right) + O(\Delta x^4). \tag{83}$$

Using Laplace transforms and the asymptotic expressions in Eqs. (57) and (58) (evaluated for $s-k$ small) we arrive at Eq. (72) for long times.

For short times we find

$$\frac{\partial n(x,t)}{\partial t} = D_\gamma^* e^{kt}\frac{\partial^{1-\nu_\gamma}}{\partial t^{1-\nu_\gamma}}\left(e^{-kt}\frac{\partial^2 n(x,t)}{\partial x^2} \right) - \chi_\gamma^* e^{kt}\frac{\partial}{\partial x}\frac{\partial}{\partial t}\left(\frac{\partial c(x,t)}{\partial x}\frac{\partial^{-\nu_\gamma}}{\partial t^{-\nu_\gamma}}(e^{-kt}n(x,t)) \right) + kn(x,t) \tag{84}$$

with ν_γ and the modified coefficients as defined previously for Model IV in Sec. II.

IV. NUMERICAL SOLUTIONS AND MONTE CARLO SIMULATIONS

It is straightforward to obtain numerical solutions of the above model equations using difference approximations. In this section we describe numerical solutions for self-chemotactic variants of the model equations and we compare the solutions with Monte Carlo simulations.

Implementation details for the Monte Carlo simulations are described in the Appendix. In the results reported here simulations were conducted on a one-dimensional lattice using the Pareto waiting-time density [Eq. (25)] with the characteristic waiting-time $\tau=0.1$, fractional exponent $\gamma=0.5$,

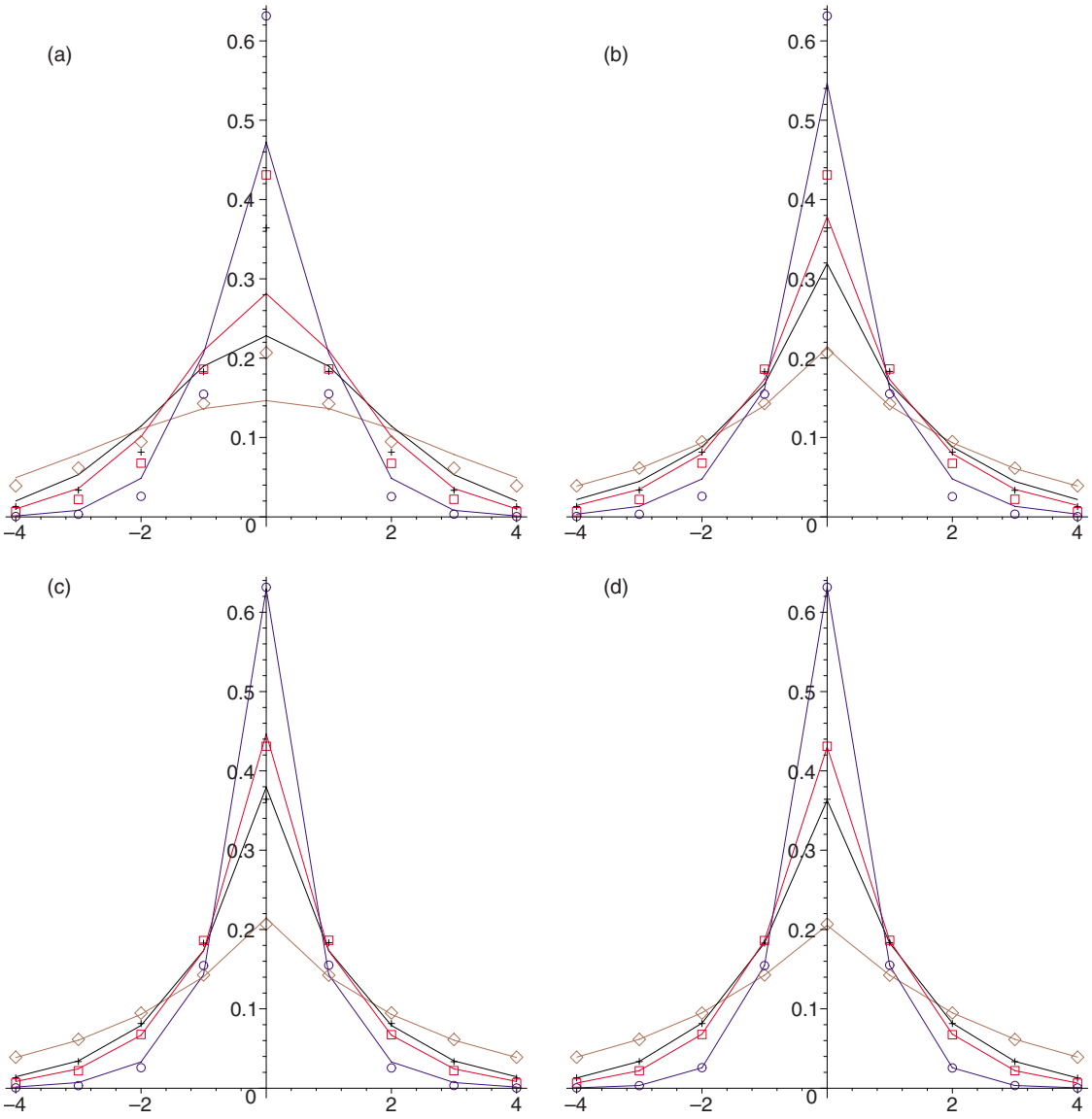

FIG. 1. (Color online) One-dimensional subdiffusive chemotaxis simulation results (circles) with $\beta=0.1$ showing the concentration profile at $t=0.4$ (blue circles), $t=2$ (red squares), $t=4$ (black crosses), and $t=20$ (brown diamonds) compared with the numerical solution of the governing equations for Models I (a), II (b), III (c), and IV (d) (solid lines). The peak height decreases with time in the solid curves.

and chemotactic sensitivity, β. The simulation results are from an average of 200 runs with 10 000 particles initially located at the origin.

As our starting point for numerical solutions of the macroscopic models we consider the discrete space variants of Models II, III, and IV given by Eq. (29), (44), and (47), respectively. A discrete space variant for Model I, analogous to the discrete space variant for Model II, is given by

$$\frac{dn_i(t)}{dt} = \frac{A_\gamma \gamma t^{\gamma-1}}{\tau^\gamma}[p_r(x_{i-1},t)n_{i-1}(t) + p_l(x_{i+1},t)n_{i+1}(t) - n_i(t)]. \tag{85}$$

The discrete space equations for Models II and III were solved using an implicit time stepping method with the fractional derivatives approximated using the L1 scheme [48] as in [49]. For Model IV, the integrals in the discrete space representation were approximated by taking the unknown concentration, $n_{i\pm1}(t)$, to be piecewise linear in time.

The numerical solutions of the discrete space equations and the Monte Carlo simulations were performed using the same space grid size and similar values for the parameters τ, γ, and β. We also chose the same initial condition (one at the origin and zero elsewhere). The constant A_γ was chosen as in Eq. (26) since we used the Pareto density, Eq. (25), in the simulations.

In Fig. 1 we compare the Monte Carlo simulation results with the numerical solution of the discrete space equations for each model with the chemotactic sensitivity parameter, $\beta=0.1$. Further results are shown in Figs. 2 and 3 for the sensitivity parameter values $\beta=1$ and $\beta=10$, respectively.

The numerical solutions for Model III [Eq. (44)] and Model IV [Eq. (47)] are in close agreement with the Monte Carlo simulations at all times. The numerical solution for

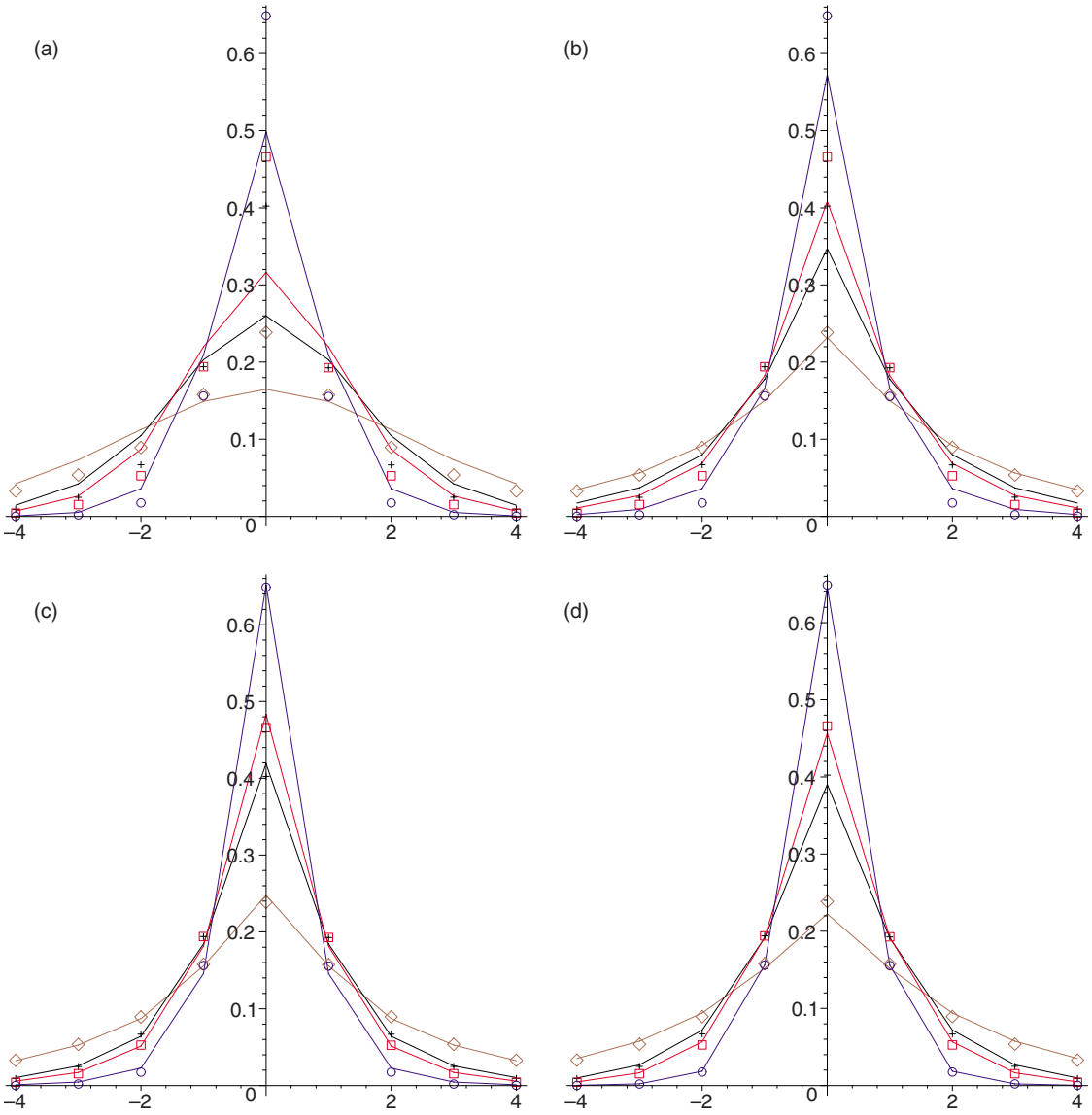

FIG. 2. (Color online) One-dimensional subdiffusive chemotaxis simulation results with $\beta=1.0$ showing the concentration profile at $t=0.4$ (blue circles), $t=2$ (red squares), $t=4$ (black crosses), and $t=20$ (brown diamonds) compared with the numerical solution of the governing equations for Models I (a), II (b), III (c), and IV (d) (solid lines). The peak height decreases with time in the solid curves.

Model II does not fit with the Monte Carlo simulations well at short times but it provides a good fit at long times ($t=20$). The numerical solution for Model I does not fit the Monte Carlo simulations well, especially for small values of β, where the predicted shape near the origin is smoother than that exhibited by the simulation data.

The closer agreement between the numerical results for Models III and IV and the Monte Carlo simulations is due to the timing of the chemotactic forcing. In Models III and IV, and in the Monte Carlo simulations the chemotactically influenced jumping probabilities are determined at the end of the waiting times, whereas in Model II they are determined at the start of the waiting times. This difference is less marked if the chemotactic concentration varies slowly in time.

Overall, the numerical solutions for Model III provide better agreement with the Monte Carlo simulations than the numerical solutions for Model IV. This better agreement can be seen at the intermediate value of $\beta=1$ in Fig. 2. This better agreement may be due to differences in numerical errors in approximating the discrete space equations for Model II and Model IV rather than due to differences between the equations themselves.

V. SUMMARY AND DISCUSSION

The correct form of the fractional Fokker-Planck equation for particles undergoing anomalous subdiffusion in an external space and time varying force field has been an open problem. In the absence of a force field, subdiffusion can be modeled with a fractional temporal derivative operating on the spatial Laplacian. For subdiffusion in a purely space dependent force field the fractional temporal derivative can be put to the left of the standard terms on the right hand side of the standard Fokker-Planck equation [13,29,31,50] as in Eq.

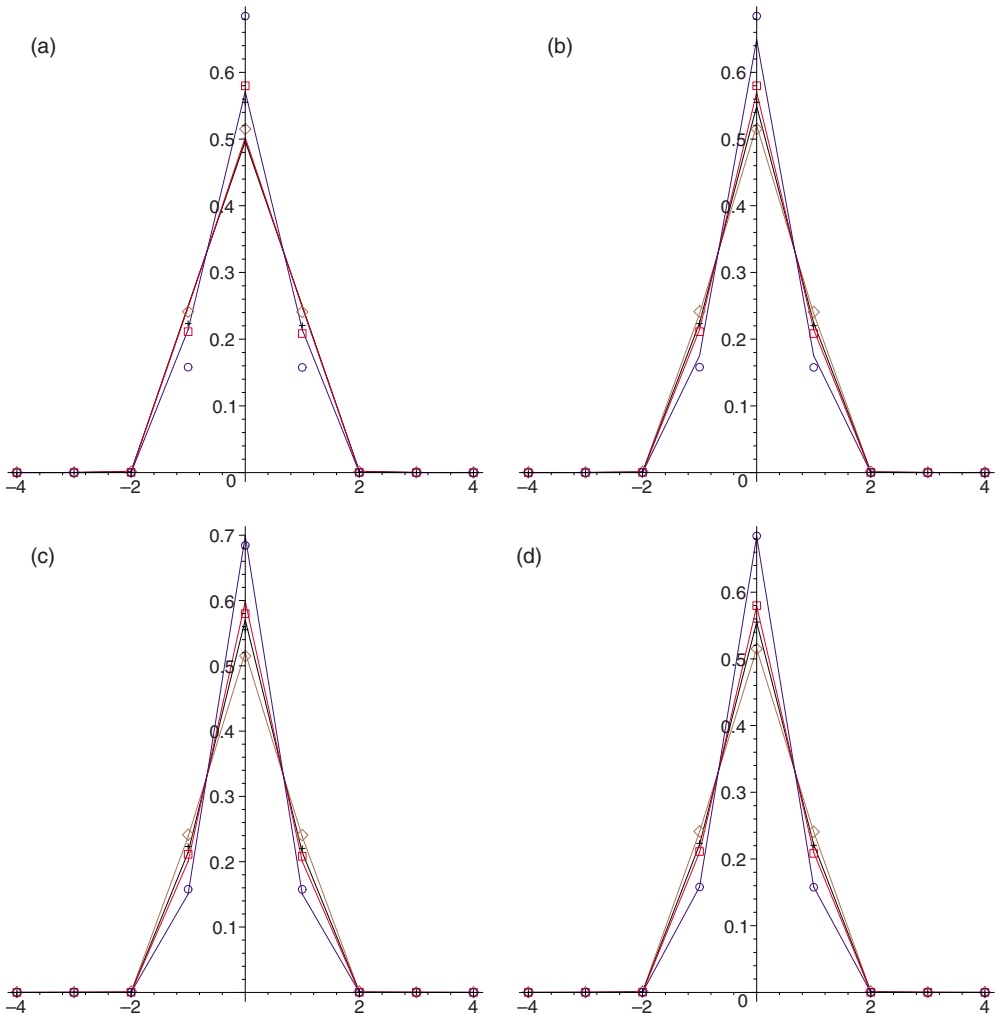

FIG. 3. (Color online) One-dimensional subdiffusive chemotaxis simulation results with $\beta=10.0$ showing the concentration profile at $t=0.4$ (blue circles), $t=2$ (red squares), $t=4$ (black crosses), and $t=20$ (brown diamonds) compared with the numerical solution of the governing equations for Models I (a), II (b), III (c) and IV (d) (solid lines). The peak height decreases with time in the solid curves.

(7). However the consensus has been that for subdiffusion in an external space-time-dependent force field the fractional temporal derivative should not operate on the force field [32–34], as in Eq. (8). The modeling is further complicated if the force itself is affected directly or indirectly by the subdiffusing particles. This is the case in fractional electrodiffusion and fractional chemotaxis diffusion, the case considered here.

In this paper we have introduced and investigated four models for particles undergoing anomalous subdiffusion in the presence of chemotactic forcing. The first being based on an *ad-hoc* extension to the fractional Brownian motion equation (Model I), two models based on continuous time random walks where concentration-dependent jump probabilities were evaluated before (Model II) or after (Model IV) the particle waiting, and a fourth model derived from a generalized master equation (Model III). Concentration-dependent jump probabilities were used to incorporate the effect of chemotaxis in discrete space representations of the models and in the Monte Carlo (MC) simulations.

Evaluating the jump probabilities prior to waiting in the CTRW formulation (Model II) resulted in a macroscopic equation (valid in the long time limit) with the fractional derivative acting upon the chemotactic gradient. Conversely, using a generalized master equation approach with the probabilities evaluated after waiting but prior to jumping gave a macroscopic equation where the fractional derivative does not act upon the gradient (Model III). The CTRW formulation with the jump probabilities evaluated after waiting (Model IV) could only be reduced to a fractional Fokker-Planck continuum equation in the asymptotic limit for long and short times. For long-times Models II and IV coincide while for short times we found Models III and IV coincide asymptotically if a Mittag-Leffler density is used.

We also introduced Monte Carlo methods for simulating anomalous subdiffusion in a chemotactic force field. In the Monte Carlo simulations the chemotactically influenced jump lengths were computed at the end of the waiting times, similar to Models III and IV. This could explain the excellent agreement we found between numerical solutions for Models III and IV and the Monte Carlo simulations. The numerical solutions for Model II also showed good agreement at long times. The numerical solutions based on the fractional

Brownian motion equation, did not agree well with the Monte Carlo results.

The fractional chemotaxis diffusion models were further generalized to incorporate linear reaction dynamics. As in previous research [44,45,51], we found that the incorporation of linear reactions required the replacement of the Riemann Liouville fractional derivative with a modified version, in addition to including the linear reaction term.

The essential difference between the CTRW models for chemotaxis with subdiffusion that were considered in this paper is the timing of the detection and response to the chemotactic gradient. In Model II the organism or cell detects the chemotactic gradient but is then trapped before it responds. In Model III the organism or cell detects and responds to the chemotactic gradient after having been trapped.

Recently it has been established that the chemotactic motion of many cells is directed by internal Ca^{2+} gradients [52] which are themselves established as the cell moves through an external chemotactic gradient. If the cell becomes trapped then upon release it will initially continue in the direction of the internal Ca^{2+} gradient, corresponding to the external chemotactic gradient at the pre-trapping time. Model II could be used to model this chemotactic motion with subdiffusion.

Other organisms or cells have spatially separated sensor regions that allow for instantaneous detection and response to chemical gradients [53]. For example crustaceans have chemosensory hairs along their appendages. The motile response to chemical gradients detected by spatially separated sensors is referred to as tropotaxis. This type of chemotaxis, with subdiffusion, would be better modeled by Model III (or Model IV).

In our application of CTRWs to chemotaxis with subdiffusion we considered the simplest case in which the subdiffusion arises from the physical and biological constraints of the medium, for example from traps or from effective crowding by other molecules. More generally one could consider models in which the chemotaxis is itself affecting the characteristics of the subdiffusion. One way to model this behavior would be to consider a waiting-time density (and survival probability) with the time scale parameter τ and the scaling exponent γ taken to be functions of the concentration of the chemoattractrant. The models considered in this paper provide a foundation for such future studies.

The fractional chemotaxis diffusion equations developed in this paper provide a new class of models for biological transport influenced by chemotactic forcing, macromolecular crowding and traps. We have recently generalized these models to include arbitrary space-and-time dependent forces [54].

ACKNOWLEDGMENT

This work was supported by the Australian Research Council.

APPENDIX: MONTE CARLO SIMULATIONS

In this section we briefly describe the Monte Carlo method used to simulate chemotaxis on a periodic one-dimensional lattice with long-tailed waiting-time density (subdiffusion). For each simulation run, the following steps are conducted

(1) Set the number of grid points, simulation time, and the initial number of particles.

(2) Initialize the parameters for the waiting-time and jump-length probability density functions.

(3) Set up the initial particle positions.

(4) For each particle generate a random waiting time, δt, (time of the first jump).

(5) Initialize the output time $t_{out}=\Delta t$.

(6) Find the time of the next jump by finding the minimum of all jumping times, t_{jump}.

(7) If $t_{jump}>t_{out}$ then go to step (8) otherwise go to step (9).

(8) Store the current particle positions. Add Δt to t_{out}. If t_{out} exceeds the simulation time then simulation ends otherwise go to step (7).

(9) Generate a random jump length, δx (see below).

(10) Generate a new waiting time and update this particle's jumping time and position ($t_{jump}=t_{jump}+\delta t$, $x_{new}=x_{old}+\delta x$).

(11) Go to step (6).

1. Generation of waiting times

The waiting times for each particle/jumper were generated by comparing a uniform random number, $r\in(0,1)$, with the cumulative probability function of the waiting-time density. We use the Pareto density [Eq. (25)] as the density which has used by Yuste, Acedo, and Lindenberg [41]. The generated waiting-time is given as

$$\delta t=\tau((1-r)^{-1/\gamma}-1), \tag{A1}$$

where $r\in(0,1)$ is a uniform random number.

2. Generation of jump distances

The jump distance for each particle/jumper is generated by comparing an uniform random number, $r\in(0,1)$, with the cumulative probability function of the jump-length density.

For the simulations we use the jump-length probability density nearest neighbor jumps only,

$$\delta x=\begin{cases}-\Delta x, & 0\le r<p_l,\\ \Delta x, & p_l\le r<1\end{cases} \tag{A2}$$

where Δx is the grid spacing and $p_l=p_l(x_i,t)$ is the probability of jumping to the left given previously in Eqs. (12) and (14).

To evaluate the probabilities of jumping to the left or right for Eq. (A2), requires the approximation of the chemoattractant concentration, $c(x_i,t)$, in Eq. (14). This is estimated by the proportion of chemoattractant particles at the grid point, x_i, compared with the total number of particles in the system.

[1] G. Wadhams and J. Armitage, Nat. Rev. Mol. Cell Biol. **5**, 1024 (2004).
[2] P. Van Haastert and P. Devreotes, Nat. Rev. Mol. Cell Biol. **5**, 626 (2004).
[3] M. Owen, T. Alarcon, P. Maini, and H. Byrne, J. Math. Biol. **58**, 689 (2009).
[4] M. J. Saxton, Biophys. J. **92**, 1178 (2007).
[5] J. Dix and A. Verkman, Annu. Rev. Biophys. **37**, 247 (2008).
[6] R. N. Ghosh and W. W. Webb, Biophys. J. **66**, 1301 (1994).
[7] T. J. Feder, I. Brust-Mascher, J. P. Slattery, B. Baird, and W. W. Webb, Biophys. J. **70**, 2767 (1996).
[8] M. J. Saxton, Biophys. J. **70**, 1250 (1996).
[9] E. D. Sheets, G. M. Lee, R. Simson, and K. Jacobson, Biochemistry **36**, 12449 (1997).
[10] P. R. Smith, I. E. G. Morrison, K. M. Wilson, N. Fernandez, and R. J. Cherry, Biophys. J. **76**, 3331 (1999).
[11] E. B. Brown, E. S. Wu, W. Zipfel, and W. W. Webb, Biophys. J. **77**, 2837 (1999).
[12] R. Simson, B. Yang, S. E. Moore, P. Doherty, F. S. Walsh, and K. A. Jacobson, Biophys. J. **74**, 297 (1998).
[13] R. Metzler and J. Klafter, Phys. Rep. **339**, 1 (2000).
[14] M. J. Saxton, Biophys. J. **81**, 2226 (2001).
[15] M. Weiss, H. Hashimoto, and T. Nilsson, Biophys. J. **84**, 4043 (2003).
[16] D. S. Banks and C. Fradin, Biophys. J. **89**, 2960 (2005).
[17] E. Ozarslan, P. J. Basser, T. M. Shepherd, P. E. Thelwall, B. C. Vemuri, and S. J. Blackband, J. Magn. Reson. **183**, 315 (2006).
[18] E. Keller and L. A. Segel, J. Theor. Biol. **30**, 225 (1971).
[19] S. Adelman, J. Chem. Phys. **64**, 124 (1976).
[20] K. G. Wang and C. W. Lung, Phys. Lett. A **151**, 119 (1990).
[21] K. G. Wang, L. K. Dong, X. F. Wu, F. W. Zhu, and T. Ko, Physica A **203**, 53 (1994).
[22] E. Montroll and G. Weiss, J. Math. Phys. **6**, 167 (1965).
[23] H. Scher and M. Lax, Phys. Rev. B **7**, 4491 (1973).
[24] E. Lutz, Phys. Rev. E **64**, 051106 (2001).
[25] Y. He, S. Burov, R. Metzler, and E. Barkai, Phys. Rev. Lett. **101**, 058101 (2008).
[26] A. Lubelski and J. Klafter, Biophys. J. **94**, 4646 (2008).
[27] M. Magdziarz, A. Weron, K. Burnecki, and J. Klafter, Phys. Rev. Lett. **103**, 180602 (2009).
[28] B. I. Henry, T. A. M. Langlands, and P. Straka, in *Complex Physical, Biophysical and Econophysical Systems: World Scientific Lecture Notes in Complex Systems*, edited by R. L. Dewar and F. Detering (World Scientific, Singapore, 2010), Vol. 9, pp. 37–90.
[29] E. Barkai, R. Metzler, and J. Klafter, Phys. Rev. E **61**, 132 (2000).
[30] I. M. Sokolov and J. Klafter, Phys. Rev. Lett. **97**, 140602 (2006).
[31] I. M. Sokolov, Phys. Rev. E **63**, 056111 (2001).
[32] E. Heinsalu, M. Patriarca, I. Goychuk, and P. Hänggi, Phys. Rev. Lett. **99**, 120602 (2007).
[33] A. Weron, M. Magdziarz, and K. Weron, Phys. Rev. E **77**, 036704 (2008).
[34] E. Heinsalu, M. Patriarca, I. Goychuk, and P. Hänggi, Phys. Rev. E **79**, 041137 (2009).
[35] B. I. Henry, T. A. M. Langlands, and S. L. Wearne, Phys. Rev. Lett. **100**, 128103 (2008).
[36] T. A. M. Langlands, B. I. Henry, and S. L. Wearne, J. Math. Biol. **59**, 761 (2009).
[37] A. Stevens, SIAM J. Appl. Math. **61**, 172 (2000).
[38] G. Margolin, Physica A **334**, 46 (2004).
[39] E. Scalas, R. Gorenflo, F. Mainardi, and M. Raberto, Fractals **11**, 281 (2003).
[40] I. Podlubny, *Fractional Differential Equations*, Mathematics in Science and Engineering Vol. 198 (Academic, New York and London, 1999).
[41] S. B. Yuste, L. Acedo, and K. Lindenberg, Phys. Rev. E **69**, 036126 (2004).
[42] A. V. Chechkin, R. Gorenflo, and I. M. Sokolov, J. Phys. A **38**, L679 (2005).
[43] I. M. Sokolov and J. Klafter, Chaos, Solitons Fractals **34**, 81 (2007).
[44] B. I. Henry, T. A. M. Langlands, and S. L. Wearne, Phys. Rev. E **74**, 031116 (2006).
[45] I. M. Sokolov, M. G. W. Schmidt, and F. Sagués, Phys. Rev. E **73**, 031102 (2006).
[46] A. Yadav and W. Horsthemke, Phys. Rev. E **74**, 066118 (2006).
[47] S. Fedotov, Phys. Rev. E **81**, 011117 (2010).
[48] K. Oldham and J. Spanier, *The Fractional Calculus: Theory and Applications of Differentiation and Integration to Arbitrary Order*, Mathematics in Science and Engineering Vol. 111 (Academic Press, New York and London, 1974).
[49] T. A. M. Langlands and B. I. Henry, J. Comput. Phys. **205**, 719 (2005).
[50] R. Metzler, E. Barkai, and J. Klafter, Europhys. Lett. **46**, 431 (1999).
[51] T. A. M. Langlands, B. I. Henry, and S. L. Wearne, Phys. Rev. E **77**, 021111 (2008).
[52] R. A. Brundage, K. E. Fogarty, R. A. Tuft, and F. S. Fay, Science **254**, 703 (1991).
[53] D. B. Dusenbery, *Sensory Ecology: How Organisms Acquire and Respond to Information* (W. H. Freeman and Co., New York, 1992).
[54] B. I. Henry, T. A. M. Langlands, and P. Straka, e-print arXiv:1004.4053.